

Invited talk given at the International  
Symposium on Superheavy Elements,  
Lubbock, TX, March 9 - 11, 1978

LBL-7705

*conf-780333-6*

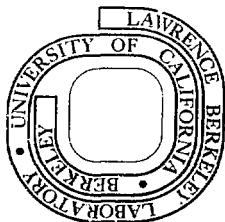
**MASTER**

EXPERIMENTAL PROSPECTS FOR THE SYNTHESIS AND  
DETECTION OF SUPERHEAVY ELEMENTS

J. Michael Nitschke

March 28, 1978

Prepared for the U. S. Department of Energy  
under Contract W-7405-ENG-48

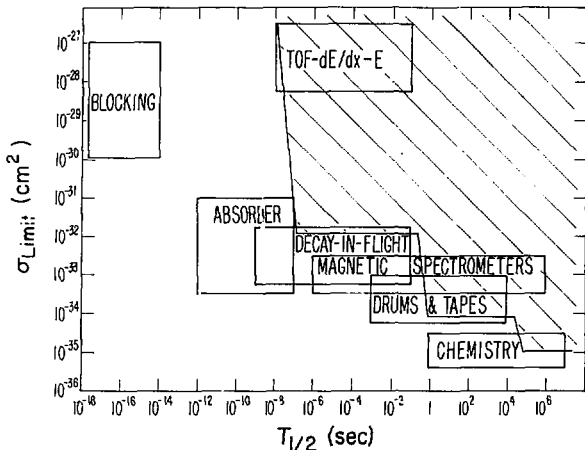


LBL-7705

DISTRIBUTION OF THIS DOCUMENT IS UNLIMITED

LEGAL NOTICE

This report was prepared as an account of work sponsored by the United States Government. Neither the United States nor the Department of Energy, nor any of their employees, nor any of their contractors, subcontractors, or their employees, makes any warranty, express or implied, or assumes any legal liability or responsibility for the accuracy, completeness or usefulness of any information, apparatus, product or process disclosed, or represents that its use would not infringe privately owned rights.



XBL 783 - 2433

Figure 2

limit; (2) recoil ranges which limit the production rate; (3) low beam intensities for very heavy ions; (5) heat dissipation in the target which limits the usable beam intensity and consequently the production rate; (6) sufficiently neutron-rich high  $Z$  target materials which are only available in submicrogram quantities (Table 1); and last but not least, (7) SHE production has to compete for beam time with other interesting physics.

At present it is therefore more profitable to consider the exploration of shorter half lives and higher cross sections as well as reaction mechanisms other than complete fusion. Starting with the longest half lives we will briefly discuss detection schemes which could be used in further searches for SHE.

#### B. DETECTION METHODS IN THE SEARCH FOR SHE

$T_{1/2} \geq 1$  sec: Chemical techniques can be sped up and automated [Hu 75] to the extent that half lives of the second range can be studied [GSI 77]. The advantages are an unambiguous  $Z$ -identification, low background and high sensitivity since thick, water-cooled targets can be used. A somewhat related method is thermochromatography [Ba 78] which can operate in the same half live range but is more ambiguous.

TABLE I. Availability of neutron-rich target materials.

| Isotope   | Quantity            |                         |  |
|---|---------------------|-------------------------|--|
|   | Routinely available | Exceptionally available | Possibly available in the future                     |
| $^{244}\text{Pu}$                                 | >100 mg             | > 1000 mg               | --   |
| $^{248}\text{Cm}$                                 | 10 mg               | 100 mg                  | --   |
| $^{250}\text{Cm}$                                 | $4.10^{12}$ atoms   | $8.10^{10}$ atoms       | $\approx 40$ mg <sup>*</sup>                         |
| $^{249}\text{Bk}$                                 | 5 mg                | 30 mg                   | --   |
| $^{249}\text{Cf}$                                 | 1 mg                | 25 mg                   | --   |
| $^{250}\text{Cf}$ (mixed, 90% $^{252}\text{Cf}$ ) | 10 mg               | 100 mg                  | 40 mg <sup>*</sup>                                   |
| $^{251}\text{Cf}$                                 | --                  | --                      | 6 mg <sup>*</sup>                                    |
| $^{252}\text{Cf}$                                 | 10 mg               | 100 mg                  | --   |
| $^{254}\text{Cf}$                                 | --                  | $5.10^4$                | $(5.10^{12}$ atoms) <sup>†</sup>                     |
| $^{253}\text{Es}$ (isotopically pure)             | 50 $\mu\text{g}$    | 200 $\mu\text{g}$       | --   |
| $^{253}\text{Es}$ (mixed)                         | 50 $\mu\text{g}$    | 700 $\mu\text{g}$       | --   |
| $^{254}\text{Es}$                                 | 1.5 $\mu\text{g}$   | 5 $\mu\text{g}$         | 25 $\mu\text{g}$<br>(n-irrad. of $^{253}\text{Es}$ ) |
| $^{258}\text{Es}$                                 | --                  | $10^{11}$ atoms         | --   |
| $^{257}\text{Fm}$                                 | $1.10^3$ atoms      | $4.10^3$ atoms          | --   |
| $^{258}\text{Md}$                                 | 0                   | 0                       | --   |

\* "Hutch" Heavy Element Experiment (Ecc 69).

† Decayed.

$T_{1/2} \geq 100$  msec: This is the domain where the He-jet surpasses most other methods, witnessed by the fact that it has led to the discovery of several new elements [Ch 74]. In the future it might be possible to combine the He-jet with a mass separator to obtain A and Z identification. Z-identification would be possible through the detection of characteristic x-rays.

$T_{1/2} \geq 1$  msec: Tape systems and fast spinning disks and drums near the target allow the rapid detection of SF and  $\alpha$ -decay. This method is, however, very crude since it is not capable of any direct A or Z identification and is plagued with a high background for  $\alpha$ -detection.

$T_{1/2} \geq 1$   $\mu\text{sec}$ : This is the domain of a wide variety of instruments based on magnetic and/or electric deflection of target recoils. Principal representatives are the Wien filter (or velocity filter), the magnetic spectrometer and the gas-filled separator. Drawbacks of these instruments are their sensitivity to the charge distribution of the recoils; they have a small solid angle (1-10 msr), are not very flexible, and expensive.

$T_{1/2} \geq 10$  ns: For this time scale, Time-of-Flight (TOF), and dE/dx-E telescope techniques are well suited. Almost all information about deep inelastic reactions has

been obtained by these methods; they are flexible, inexpensive and give moderate A and Z resolution; suffer however from high background and small solid angles.

$T_{1/2} \geq 1 \text{ ns}$ : Decay in flight (DIF) techniques, an example of which is shown in Fig. 3, have led to the shortest time limits for SHE formation so far (Fig. 1). Background effects, however, limit the sensitivity at present to about 1 nb.

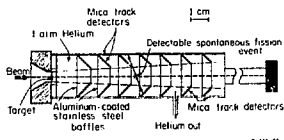


Figure 3

$T_{1/2} \geq 1 \text{ ps}$ : The flight path of recoils with half lives in the pico-second range is tens of microns. A half-life determination can therefore be based on the observation whether they traverse an absorber deposited directly on the target before undergoing SF decay. Fission fragments from the target material are suppressed by making the absorber sufficiently thick.

$T_{1/2} \geq 1 \text{ as}$  ( $10^{-18}$  seconds): The only detection method known for this time scale is the blocking technique (Fig. 4) [Gi 74]. It is restricted to target materials which can be obtained as single crystals and is rather insensitive due to the small solid angle of the position sensitive detector.

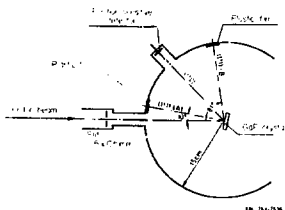


Figure 4

### C. ALTERNATE PRODUCTION MODES FOR SHE

The widest ranging search for SHE has been based on the assumption that they can be formed in compound nucleus reactions. The most favorable combination,  $^{48}\text{Ca} + ^{248}\text{Ca}$ , has been explored thoroughly [Hu 78] with negative results. This lack of success can be ascribed to one or all of the following reasons [Ni 78]: (1) the half-lives are shorter than predicted; (2) the excitation energies and angular momenta are too high and the SHE disintegrates before forming a compound system; (3) the extrapolation of the shell model into the region of  $Z=114$  is incorrect and SHE do not exist. A slim chance for future searches would be the use of still heavier targets like  $^{250}\text{Cm}$  but its availability is limited as shown in Table I. Also targets like Es become increasingly difficult to handle due to their high specific radioactivity. In the following we will therefore address the question of producing heavy and superheavy elements with other than complete fusion reactions, in particular, deep inelastic reactions.

A representative sample of this reaction mechanism is shown in Fig. 5 where the total kinetic energy (TKE) of the fragments in the center of mass system is plotted as a function of the center of mass angle of the projectile-like fragment for different reactions (these plots have become known as Wilczynski plots). All six reactions have been studied at GSI [Sa 77]. Two horizontal lines have been added indicating the total available kinetic energy and the Coulomb repulsion energy for spherical fragments; the vertical line marks the grazing angle. It is evident that the six reactions are of quite different nature: in the Kr-Er case a large fraction of the total cross section goes to forward angles and the TKE loss exceeds the Coulomb repulsion energy. This has been interpreted as orbiting effect of the projectile around the target nucleus. The lower repulsion energy is due to deformations of the fragments. The Xe-Sn shows both effects less pronounced while the Xe-Au reaction (Fig. 5c) exhibits a strong angular focusing effect [Schr 77] where the intermediate double nucleus decays at approximately the grazing angle independent of angular momentum. For the heavier system, Pb-Pb, a monotonic increase of the scattering angle with increasing TKE loss is observed and the fragments part with the mutual Coulomb repulsion energy. In the U-systems the TKE for most fragments is above the Coulomb energy.

For the purpose of producing heavy and superheavy elements a plot of the TKE loss as a function of the Z of the projectile-like fragment is of great importance. This is shown in Fig. 6 for the same reactions. The principle feature for the three "light" reactions

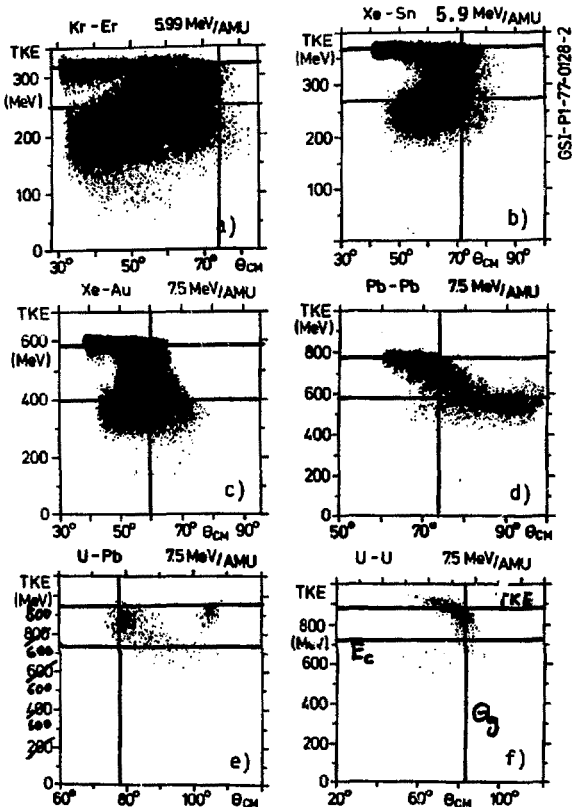
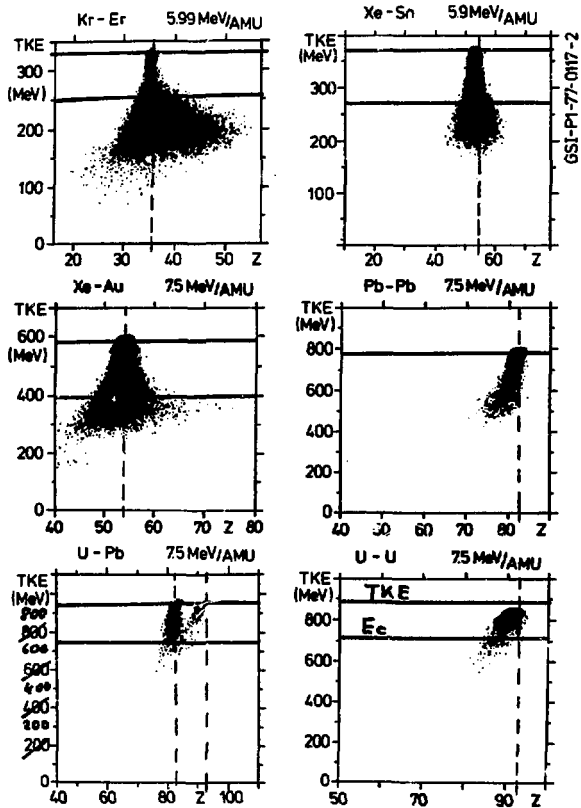


Figure 5



XBL 783-7447

Figure 6



is that the variance of the Z distribution increases with increasing TKE loss. This has been explained in a diffusion model [Mo 76][Wo 78] as an increased interaction time witnessed by the angular distributions (Fig. 5). The heavier systems show a highly asymmetric Z-distribution due to sequential fission. Figure 7 gives a more qualitative picture of the increase of the variance  $\sigma_Z^2$  with TKE loss for the reaction  $^{136}\text{Xe} + ^{209}\text{Bi}$  [Schr 76]. The cross sections for different elements as a function of TKE (Fig. 8) shows a feature which will be of importance in the discussion of a spectrometer for the deep inelastic reaction products: the variance of the total kinetic energy distribution becomes smaller for increasing proton removal or pickup. The other feature possibly of importance for the synthesis of SHE can be seen in the reaction Xe + Au (Fig. 9) [Sa 77]: the Z-distributions at low TKE loss are successfully described by Gaussians but with increasing TKE loss, a driving force towards the closed proton shell at Z=50 manifests itself (which would correspond to a complementary force for the gold nucleus towards Z=82).

Huizenga et al have found a "universal" relationship between the TKE loss and the variance of the Z-distributions as shown in Fig. 10 [Hu 76]:

$$\ln(E_0/E) \propto \sigma_Z^2$$

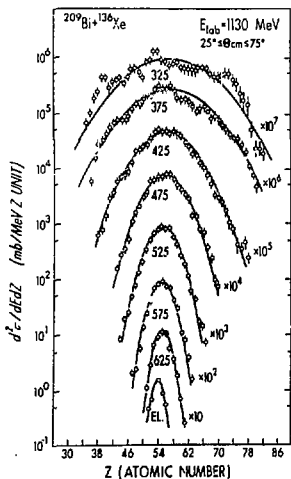


Figure 7

XBL 783-7455

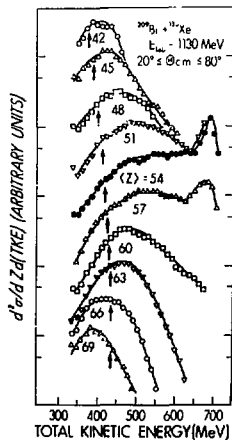


Figure 8

XBL 781-7440

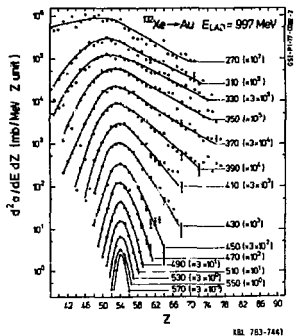


Figure 9

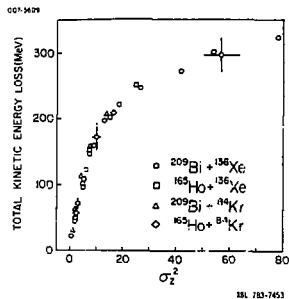


Figure 10

here  $E_0 = E_{c.m.} - E_{coul}$ , and  $E = E_{c.m.} - E_{loss} - E_{coul}$ . This relationship is obviously detrimental to the production of new elements since in order to obtain a large  $\sigma_Z^2$ , large amounts of energy have to be dissipated which will result in a large excitation energy of the heavy fragment and subsequent fission.

Two factors, however, might save the situation: Hildenbrand et al have found that the curve shown in Fig. 10 does not apply to the reaction U+U; this is shown in Fig. 11 [Hi 77]: for a given TKE loss a much wider charge distribution is obtained. If this trend continues the acceleration of the heaviest elements and the bombardment of the heaviest targets will be of great importance. The second factor which could increase the cross sections for reactions which require large proton transfer has already been pointed out with reference to Fig. 9: if target and projectile can be combined so that the exchange of  $x$  protons leads to closed proton shells in the two fragments, an enhancement of the SHE cross section can be expected. This effect, however, has thus far only been demonstrated for relatively high TKE losses and large cross sections. It should be pointed out that shell closure or near shell closure has to be achieved for both fragments. This can be seen in the Xe+Bi reaction (Fig. 7) which is unfavorable for showing this effect since the target and projectile are already near closed proton and neutron shells and consequently no shell effect for the quasi-projectile at  $Z=50$  or  $Z=82$  is observed. Deviations from a diffusion model towards higher cross sections at large proton transfers are, however, also present in this reaction as shown in Fig. 12 [Wo 78]. The left wing can be attributed to fission from the heavy fragment while the right wing is as yet unexplained.

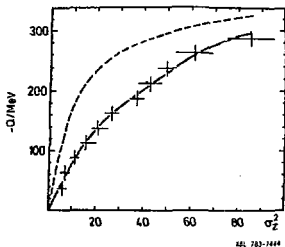


Figure 11

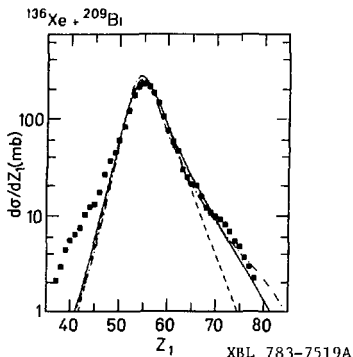


Figure 12

Another effect which could have considerable bearing on the production of new elements via deep inelastic reactions has been observed at GSI in a comparison between the Pb+Pb and the U+U reaction (Fig. 13). If the primary Z distribution around the target/projectile is identical in both cases, the production of  $Z=87$  which is in the middle between Pb and U, should be similar, however, it is a factor 40 higher for U+U. Two possible explanations for this effect have been put forward [Sa 77]: (1) the emission of light charged particles during or after the primary fragmentation, or (2) a mass transfer at lower excitation energies (!) related to the fact that U is deformed and Pb is not. It should, however, be pointed out that a comparison of only the proton number is not quite appropriate since the mass to charge ratios in the two reactions are different and fragments near  $Z=87$  created in the U+U reaction have on the average 4.4 additional neutrons available for "cooling," which corresponds to a reduction in excitation energy of about 33 MeV.

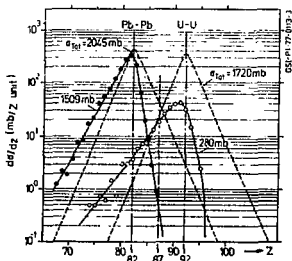


Figure 13

The decrease in "peak" cross section when going from Pb+Pb to U+U (Fig. 13) is of great concern when heavy targets for the production of new elements are considered. It is presently unknown whether or not during the collision of very heavy nuclei the time scale for fission is short compared to the time available for the diffusion processes.

Significant information about the proton-rich side of the target-projectile diffusion process has been obtained through chemical studies at ANL, GSI, and LBL. Figure 14 shows the production of transuranium elements for different deep inelastic reactions. Table II includes more recent information from GSI and the cross sections are presented in a form where the  $^{136}\text{Xe} + ^{238}\text{U}$  reaction is normalized to 1. A substantial increase in cross sections is observed for heavier projectiles ( $^{238}\text{U}$ ) and heavier targets ( $^{248}\text{Cm}$ ). The combination of the heaviest target with the heaviest beams will be discussed presently.

TABLE II. Production ratios of selected isotopes via deep inelastic reactions.

| Reaction                            | Energy (MeV/A) | $^{242}\text{Cm}$ | $^{250}\text{Cf}$ | $^{255}\text{Bk}$ | $^{256}\text{Fm}$                        | Reference |
|-------------------------------------|----------------|-------------------|-------------------|-------------------|--|-----------|
| $^{40}\text{Ar} + ^{238}\text{U}$   | 7.2            | 17                | —                 | —                 | —  | LBL       |
| $^{84}\text{Kr} + ^{238}\text{U}$   | 7.2            | 11                | 2                 | 0.02              | —  | LBL       |
| $^{136}\text{Xe} + ^{238}\text{U}$  | 8.3            | 1                 | 1                 | 1                 | 1<br>( $\approx 10^{-34} \text{ cm}^2$ ) | K. Wolf   |
| $^{238}\text{U} + ^{238}\text{U}$   | 7.5            | 30                | 2000              | 50                | 6  | J. Kratz  |
| $^{248}\text{Cm} + ^{248}\text{Cm}$ | 8.5            | —                 | 67                | 15                | 1300                                     | LBL       |

It is useful for the calculation of SHE cross sections to get a very rough estimate of the average excitation energy of the heaviest elements produced in deep inelastic collisions. Kratz et al [Kr 78] have measured the cross section for the formation of  $^{254}\text{Fm}$  in the  $^{238}\text{U} + ^{238}\text{U}$  reaction in a thick target. The bombarding energy ranged from the Coulomb barrier to 7.5 MeV/A; and the cross section obtained is  $2 \times 10^{-33} \text{ cm}^2$ .

The reaction can schematically be written as  $^{238}\text{U}(^{238}\text{U}, ^{222}\text{Po}^*)^{254}\text{Fm}^*$ . From Fig. 13 and 15 we can deduce the cross section  $d\sigma/dz$  for TKE losses of  $\leq 100$  MeV as approximately 8 mb/z-unit at  $Z=92$ . The measured cross section for  $^{254}\text{Fm}$  is lower by a factor ( $\eta = 2 \times 10^{-33} / 8 \times 10^{-27} = 2.5 \times 10^{-7}$ ). Under the assumption that the proton number distribution is Gaussian  $\eta$ , related to the charge difference  $\Delta Z$ , and the variance

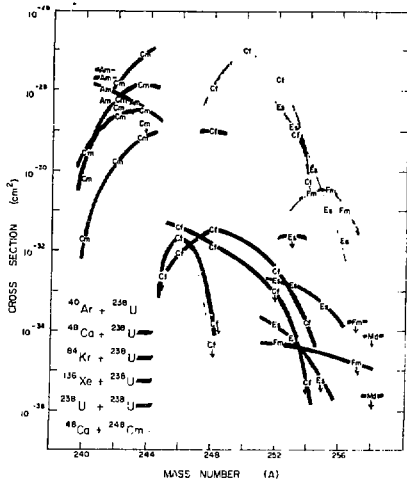


Figure 14

CBB 779-8447

of the charge distribution  $\sigma_z^2$  via

$$\sigma_z^2 = \frac{(\Delta Z)^2}{2 \ln \eta}$$

In this case:  $\sigma_z^2 = -8^2/2 \times \ln(2.5 \times 10^{-7}) = 2.1$ . From Fig. 11 we know that this variance corresponds to a TKE loss of about 17 MeV. Only part of this energy results in excitation of the fragments since the reaction Q-value is negative: in the case of  $^{238}\text{U}(^{238}\text{U}, ^{222}\text{Po}^*)^{254}\text{Fm}$ ,  $Q = -9$  MeV. This results in a total excitation energy of 8 MeV, which is distributed proportional to the mass of the fragments: the  $^{254}\text{Fm}$  nucleus receives about 4.3 MeV. This is substantially lower than the calculated fission barrier [Ts 70] and the average fission probability for this nucleus is practically zero.

#### D. ESTIMATES FOR THE PRODUCTION OF SUPERHEAVY ELEMENTS VIA DEEP INELASTIC REACTIONS

The previous estimate of the excitation energy of  $^{254}\text{Fm}$  underlines again the importance of a low excitation energy in the final nucleus in order for it to survive fission. It seems, in principle, possible to obtain lower excitation energies in deep inelastic collisions than in compound nucleus reactions. The excitation energies reached in compound reactions for SHE formations with targets like  $^{248}\text{Cm}/^{244}\text{Pu}$  and  $^{48}\text{Ca}$  as projectile have

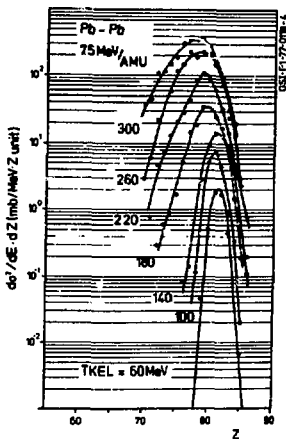


Figure 15

XBL 783-7449 A

been above 30 MeV and this could be one of the reasons why SHE have not been observed.

In the following production cross sections of SHE will be estimated without considering details of angular momentum and particle evaporation explicitly. The calculations are, however, based on experimental cross sections which include these effects. From results obtained at GSI and presented in Fig. 15 it is assumed that for low enough TKE loss -- which corresponds to low excitation of the fragment -- neutron evaporation rather than fission becomes a significant decay channel. This is observed in Fig. 15 as a transition from very asymmetric distributions at high TKE losses to near Gaussians at low TKE loss. For the following calculations it is therefore assumed that the Gaussian character of the distribution continues up to the proton shell closure in the SHE region (!).

We consider as an example the reaction  $^{238}_{\text{U}}(^{238}_{\text{U}}, ^{181}_{\text{Yb}})^{295}_{114}$ \*: for a relative fission width  $\Gamma_f/(\Gamma_f + \Gamma_n)$  of 50%, the excitation energy of the  $^{295}_{114}$  nucleus is predicted to be about 30 MeV [No 72]. Assuming partition of the total available excitation energy according to mass, the Yb nucleus carries 18 MeV. The total fragment excitation energy is therefore 48 MeV. The Q-value for the above reaction is -55 MeV, so that a TKE loss of 103 MeV can be tolerated. According to Fig. 11 this corresponds to a variance of the charge distribution of  $\sigma_Z^2 = 14$ . The cross section for  $^{295}_{114}$

can then be calculated from  $\sigma(114) = \sigma_0(92) \exp(-(\Delta Z)^2/2 \times \sigma_z^2)$  where  $\sigma_0(92)$  is taken from Fig. 13 and Fig. 15. For a TKE "window" of  $\pm 10$  MeV,  $\sigma_0(92) = 4$  mb, and with  $\Delta Z = 22$  we obtain  $\sigma(114) = 1 \times 10^{-34}$  cm<sup>2</sup>. For other target projectile combinations the cross sections have been calculated in a similar way and compiled in Table III. It has to be pointed out that the precise knowledge of the TKE( $\sigma_z^2$ ) function is of crucial importance: if the "universal" (dashed) curve (Fig. 11) as proposed by Huizenga were correct, (114) would be lowered by sixteen (!) orders of magnitude. The calculated cross section is about two orders of magnitude lower than the present experimental limit [Hi 77]. It is, however, possible to increase the cross sections through the use of heavier targets and heavier projectiles as shown in Table III. The most "realistic" reaction is  $^{238}\text{U} + ^{248}\text{Cm}$  with a calculated cross section of 0.2 nb for a SHE excitation energy of 30 MeV and a relative fission width of 50%. The "ultimate" reaction in

TABLE III. Deep inelastic reactions for the production of heavy and superheavy elements.

| Reaction | Projectile        | Target            | Product           | Q-value (MeV) | Product excitation energy (MeV) | Cross section (cm <sup>2</sup> ) | $\Gamma_f/\Gamma_f+\Gamma_n$ (per step) | Reference  |
|----------|-------------------|-------------------|-------------------|---------------|---------------------------------|----------------------------------|---|--|
| 1        | $^{178}\text{Er}$ | $^{248}\text{Cm}$ | $^{293}114$       | -90           | $10 \pm 10$                     | $2 \cdot 10^{-33}$               | $10^{-3}$                               | Based on $^{116}\text{Xe} + ^{208}\text{Bi}$ [Schr 77] |
|          | $^{170}\text{Er}$ | $^{248}\text{Cm}$ | $^{291}114$       | -90           | $30 \pm 10$                     | $3 \cdot 10^{-37}$               | $8 \cdot 10^{-1}$                       |  |
| 2        | $^{238}\text{U}$  | $^{238}\text{U}$  | $^{295}114$       | -55           | $20 \pm 10$                     | $1 \cdot 10^{-36}$               | $5 \cdot 10^{-2}$                       | [Hi 77]  |
|          | $^{238}\text{U}$  | $^{238}\text{U}$  | $^{295}114$       | -55           | $30 \pm 10$                     | $1 \cdot 10^{-34}$               | $5 \cdot 10^{-1}$                       |  |
| 3        | $^{238}\text{U}$  | $^{248}\text{Cm}$ | $^{295}114$       | -30           | $10 \pm 10$                     | $2 \cdot 10^{-41}$               | $10^{-4}$                               | Based on $^{218}\text{U} + ^{238}\text{U}$ [Hi 77]     |
|          | $^{238}\text{U}$  | $^{248}\text{Cm}$ | $^{295}114$       | -30           | $20 \pm 10$                     | $3 \cdot 10^{-37}$               | $5 \cdot 10^{-2}$                       |  |
|          | $^{238}\text{U}$  | $^{248}\text{Cm}$ | $^{295}114$       | -30           | $30 \pm 10$                     | $2 \cdot 10^{-34}$               | $5 \cdot 10^{-1}$                       |  |
| 4        | $^{238}\text{U}$  | $^{249}\text{Cf}$ | $^{292}114$       | -35           | $20 \pm 10$                     | $4 \cdot 10^{-34}$               | $10^{-1}$                               |  |
| 5        | $^{244}\text{Pu}$ | $^{254}\text{Es}$ | $^{294}114$       | -24           | $30 \pm 10$                     | $2 \cdot 10^{-32}$               | $8 \cdot 10^{-1}$                       |  |
| 6        | $^{238}\text{U}$  | $^{248}\text{Cm}$ | $^{264}\text{No}$ | -7            | $5 \pm 5$                       | $2 \cdot 10^{-31}$               | --                                      | [Hi 77]  |

the future would be  $^{244}\text{Pu} + ^{254}\text{Es}$  even though only a limited amount of target material is available (c.f. Table I). The acceleration of  $^{244}\text{Pu}$  will, however, be considered seriously for the new injector at the SuperHILAC. The reaction  $^{254}\text{Es}_{99}({}^{244}\text{Pu}_{94}, {}^{204}\text{Au}_{79})^{29}$  would have the added advantage that both fragments are near closed proton and neutron shells which could lead to enhanced cross sections as discussed earlier; also Es might show a higher resistance against preequilibrium fission compared to even-even nuclei.

To test for possible shell effects with lighter projectiles, a calculation of the reaction  $^{248}\text{Cm}(^{170}\text{Er}, ^{127}\text{Sn})^{291}_{114}$  is included in Table III. Besides producing a very neutron-deficient SHE, the calculated cross sections of  $3 \times 10^{-37} \text{ cm}^2$  is below the present detection limits.\*

Despite "heroic" efforts to accelerate the heaviest ions to bombard the heaviest targets it is still possible that SHE do not exist or cannot be synthesized. It is, however, virtually certain that many new isotopes and perhaps a few new elements will be produced in deep inelastic reactions. In Table III  $^{264}\text{No}$  is given as an example: it could be synthesized with a cross section of  $0.1 \mu\text{b}$  in the reaction  $^{238}\text{U} + ^{248}\text{Cm}$ , with an excitation energy of less than 10 MeV.

#### 2. THE DETECTION OF DIC PRODUCTS

Experiments with heavy target projectile combinations have shown that in deep inelastic collisions the projectile-like fragment is emitted near the grazing angle (c.f. Fig. 5f). For typical systems with low total kinetic energy loss as discussed in the previous section this results in the target-like fragment being emitted at angles of 40 to 50 degrees in the laboratory. The rigidity of these particles -- for 8.5 MeV/A bombarding energy -- typically 1 Tm. The conical distribution of the reaction product makes it difficult to collect them with high efficiency for the study of exotic nuclei, in particular if a short separation time is of the essence as in the previously discussed case of neutron-rich isotopes of known elements. The same applies to neutron-deficient SHE in deep inelastic collisions. In the following an instrument will therefore be discussed which combines high transmission and short separation time for fragments emitted in a conical geometry. The principal of this spectrometer was suggested in 1924 [Ka 24] based on the analogy between an optical -- and a magnetic "lens" formed by a uniform magnetic field inside a coil. These lens spectrometers have since been used extensively as  $\beta$ -spectrometers even though the technical development seems to have stopped around 1965.† For the purpose of this discussion it is sufficient to consider the first order properties of a homogeneous field spectrometer. The distance  $z$  between the source and the image is given by:

$$z = 2\pi Bp/B_0$$

\*Wolf has recently estimated the cross section for the production of  $^{290}_{114}$  in the reaction  $^{136}\text{Xe} + ^{253}\text{Es}$  to  $\sim 10^{-37} \text{ cm}^2$  [Wo 77].

† A recent review including many references is given in [Me 76] and in [Si 68].



and the maximum amplitude  $r_{\max}$  inside the field is (c.f. Fig. 16)

$$r_{\max} = \frac{2B\rho}{B_0} \sin \alpha$$

where  $\alpha$  is the emission angle of the particle. Optimum resolution is obtained for emission angles around  $40^\circ$ . For a particle rigidity  $B\rho = 1 \text{ Tm}$ , a field of  $65.3 \text{ T}$ , and an emission angle of  $45^\circ$ , the principal dimensions of the solenoid are:  $z=1 \text{ m}$  and  $r_{\max} = 0.22 \text{ m}$ .

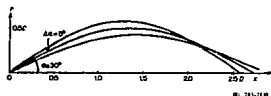


Figure 16

Such a solenoid can only be built with superconducting coils. The resolution of the lens spectrometer is on the order of 1% but can be improved through intermediate image focusing. The necessary field shape is shown in Fig. 17 [Si 68]. An instrument of similar concept is shown in Fig. 18 [He 61]. If point D is considered the target position, different detectors could be placed at point S with appropriate shielding between D and S.

In such a Heavy Ion Lens Spectrometer, the following information about a particle could be obtained: emission angle,  $B\rho$  value, time of flight,  $dE/dz$  (Z identification), and total kinetic energy. Given sufficient resolution for these quantities, particle identification in A and Z is possible.

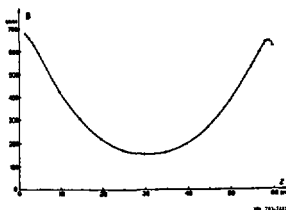


Figure 17

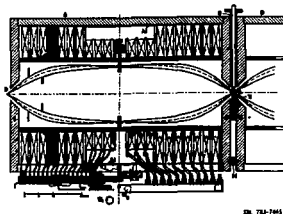


Figure 18

A drawback of any purely magnetic instrument is, of course, that the particle rigidity  $B\rho$  depends on the charge, and multiple charge states can give rise to ambiguities in the particle identification. This problem can in principle be solved by filling

the solenoid with a suitable gas at low pressure but the lower equilibrium charges will require higher fields and cause scattering problems.

#### F. CONCLUSION

The search for SHE can be extended in three directions: (1) exploration of shorter half-lives with compound nucleus reactions; (2) the use of exotic targets; and (3) the use of deep inelastic reactions. The latter possibility seems at the moment the most promising. It will also facilitate the production of new isotopes and perhaps new elements near the known region of the periodic table.

#### REFERENCES

- [Ba 78] K. Bächmann, this conference.
- [Ch 74] A. Ghiorso, J. M. Nitschke, J. R. Alonso, C. T. Alonso, M. Nurmiä, G. T. Seaborg, E. K. Hulet, and R. W. Loughheed. *Phys. Rev. Lett.* 33, 1490 (1974). *Letts.* 33, 1490 (1974).
- [Gi 74] W. M. Gibson and N. Maruyama, in "Channeling", D. V. Morgan, ed. (J. Wiley, 1974).
- [GSI 77] GSI-Report, GSI-J-1-77 (1977).
- [He 61] C. J. Herrlander and Slatis. *Ark. f. Fysik* 20, 4 (1961).
- [Hi 77] K. D. Hildebrand, H. Freiesleben, F. Pühlhofer, W.F.W. Schneider, R. Bock, D. V. Harrach, and J. H. Specht. *Phys. Rev. Lett.* 39, 1965 (1977).
- [Hu 75] E. K. Hulet, J. M. Nitschke, R. W. Loughheed, J. F. Wild, J. H. Landrum, and A. Ghiorso. *Proceedings IV Int. Transplutonium Element Symposium, Baden-Baden (1975)*.
- [Hu 76] J. R. Huizenga, J. R. Birkelund, W. U. Schröder, K. L. Wolf, and V. Viola. *Phys. Rev. Lett.* 37, 885 (1976).
- [Hu 78] E. K. Hulet, this conference.
- [Ka 24] P. Kapitza, *Proc. Cambridge Phil. Soc.* 22, part 3 (1924).
- [Kr 78] J. Kratz, private communication via H. Freiesleben (1978).
- [MI 76] M. Mladjenovic. *Development of Magnetic Beta Ray Spectrometers (Springer, 1976)*.
- [Mo 72] L. G. Moretto. *Nucl. Phys.* A180, 337 (1972).

- [Sa 77] H. Sann, A. Olmi, Y. Cirelskoglu, D. Pelte, U. Lynen, W. Stelzer, A. Gobbi, Y. Eyal, W. Kohl, R. Renfordt, I. Rode, C. Rudolf, D. Schwalm, and R. Bock. Proc. Top. Conf. Heavy Ion Collision, Fall Creek Falls (1977). p.281-308, CONF 770602.
- [Schr 76] W. U. Schröder, J. R. Birkelund, J. R. Huizenga, K. L. Wolf, J. P. Unik, and V. Viola. Phys. Rev. Lett. 36, 514 (1976).
- [Schr 77] W. U. Schröder and J. R. Huizenga. Ann. Rev. Nucl. Sci. 27, 465 (1977).
- [Si 68] K. Siegbahn, ed. Alpha-, Beta-, and Gamma-Ray Spectroscopy, Vol. 1 (North-Holland Publishing, Amsterdam, 1968).
- [Ts 70] C. F. Tsang and S. G. Nilsson. Nucl. Phys. A140, 275 (1970).
- [Wo 77] K. L. Wolf, J. P. Unik, E. P. Horwitz, C.A.A. Bloomquist, and W. Delphin. APS Meeting, Chicago, February 1977.
- [Wo 78] G. Wolschin and W. Nörenberg. Z. Phys. A284, 209 (1978).

Work supported by the U. S. Department of Energy.